Published in final edited form as:
Magn Reson Med. 2010 December ; 64(6): 1586–1591. doi:10.1002/mrm.22419.

Magnetic Field Threshold for Accurate Electrocardiography in the MRI Environment

Mihaela Jekic[1,2], **Yu Ding**[2], **Roger Dzwonczyk**[3], **Patrick Burns**[4], **Subha V. Raman**[2], and **Orlando P. Simonetti**[1,2,5,6,*]

[1] Department of Biomedical Engineering, The Ohio State University, Columbus, Ohio, USA

[2] Dorothy M. Davis Heart and Lung Research Institute, The Ohio State University, Columbus, Ohio, USA

[3] Department of Anesthesiology, The Ohio State University, Columbus, Ohio, USA

[4] Department of Veterinary Clinical Sciences, The Ohio State University, Columbus, Ohio, USA

[5] Department of Internal Medicine, Division of Cardiovascular Medicine, The Ohio State University, Columbus, Ohio, USA

[6] Department of Radiology, The Ohio State University, Columbus, Ohio, USA

Abstract

Although the electrocardiogram is known to be nondiagnostic within the bore of any high-field magnet due to the magnetohydrodynamic effect, there are an increasing number of applications that require accurate electrocardiogram monitoring of a patient inside the MRI room but outside of the magnet bore. Magnetohydrodynamic effects on the ST segment of the electrocardiogram waveform were investigated in six subjects at magnetic field strengths ranging from 6.4 mT to 652 mT at the aortic midarch, and the electrocardiogram was found to be accurate at magnetic fields below 70 mT. This corresponds to a distance of 160 cm from the isocenter and 80 cm from the bore entrance for the 1.5-T MRI system used in this study. These results can be translated to any MRI system, with knowledge of the fringe field. Accurate electrocardiogram monitoring is feasible in close proximity to the MRI magnet, such as during and after pharmacologic or exercise stress, or interventional or surgical procedures performed in the MRI room.

Keywords

magnetohydrodynamic; electrocardiogram; MRI; patient monitoring; stress test

The electrocardiogram (ECG) is known to be significantly distorted by the magnetohydrodynamic (MHD) effect and is nondiagnostic within the bore of any MRI magnet. The MHD effect results from blood flow within the static magnetic field and is most pronounced when flow is rapid and oriented perpendicular to the magnetic field, e.g., in the aortic arch (1). While techniques for R-wave detection in the MRI bore are suitable for ECG triggering of MR data acquisition (2), accurate ECG monitoring is not feasible due to MHD distortion. The magnetic field threshold at which distortion of the ECG becomes significant has not to our knowledge been previously reported. Knowledge of this threshold is important to ensure the accuracy of ECG monitoring within the fringe field inside the

*Correspondence to: Orlando P. Simonetti, 410 W 10th Ave, 527 Doan Hall, Columbus, OH 43210. simonetti.9@osu.edu.

MRI room but outside of the magnet bore. ECG monitoring is essential for the safety of critically ill or anesthetized patients undergoing MRI procedures and is also vital to several new and emerging MRI applications. The growing fields of interventional and intraoperative MRI are expanding the needs for advanced patient monitoring in the MRI magnet room. Furthermore, continuous 12-lead ECG monitoring is required during and immediately after both exercise (3) and dobutamine stress testing (4). It is important to understand the extent of the ECG distortion that may be encountered inside the MRI magnet room as these new applications become more widespread.

Stress testing by MRI, either by exercise or pharmacological stress, is an emerging application (5–9) that demands accurate ECG monitoring in the MRI room. Exercise is preferred to pharmacologic stress as a diagnostic test for ischemic heart disease (10) for several reasons, one being that exercise-induced ECG changes have diagnostic and prognostic value. However, image acquisition after stress must be completed within 60 sec of terminating exercise (11) because exercise-induced cardiac wall motion abnormalities can resolve rapidly, especially for mild stenoses (<50%) and single-vessel coronary artery disease (12). Exercise stress MRI can only be performed successfully if MRI-compatible exercise equipment is positioned on or immediately adjacent to the MRI table, necessitating accurate ECG monitoring in close proximity to the MRI magnet. Exercise-stress-induced changes in the ST segment of the ECG are indicative of ischemia, with ST depression ≥0.10 mV or ST elevation >0.10 mV considered an abnormal response (11). Unfortunately, peak aortic arch flow occurs on average between 92 and 107 ms after the R-wave (13), coincident with the ST segment, and the resulting MHD effects may mask ischemia-induced changes in the ECG. Supine (7) or upright (5) bicycle exercise inside the magnet bore precludes accurate ECG monitoring, but monitoring during bicycle exercise outside the bore on the extended MRI patient table may be feasible. ECG monitoring during exercise on a treadmill placed inside the MRI room (8), and potentially immediately adjacent to the MRI table, may also be feasible. In addition to continuous monitoring during stress testing, ECG monitoring should resume as quickly as possible after poststress imaging, ideally while the patient is still on the MRI table.

The American Heart Association (AHA) guidelines for automated electrocardiography (14) recommend that deviation from the true waveform for accurate visual assessment of the ECG signal may not exceed 0.025 mV or 5%, whichever is greater. The objective of the work presented in this paper is to determine the magnetic field threshold below which the MHD effects are within the AHA guideline for allowable ECG distortion. With details of the fringe field provided in the MRI compatibility data sheet of any clinical MRI system, the magnetic field threshold determined in this study can be translated to an acceptable distance from the magnet where accurate ECG monitoring can be performed.

MATERIALS AND METHODS

All experiments were performed on a 1.5-T MRI system (Magnetom Avanto; Siemens Medical Solutions, Malvern, PA). Using a gauss-meter axial probe (Model 420, Lake Shore Cryotonics, Westerville, OH), we measured the static magnetic field (B) at the level of the patient table in 5-cm increments from the end of the fully extended table (320 cm from isocenter) to the magnet isocenter. Since the aortic arch flow is the primary source of the MHD effect (1)(15), we used MRI scout images to find the distance from the aortic arch to the isocenter in all subjects in order to determine the magnetic field at the aortic arch at various table positions. An estimate of the induced MHD voltage across the aorta may be expressed as (1):

$$\mathbf{V}=\int \mathbf{u} \times \mathbf{B} \cdot d\mathbf{L} \quad [1]$$

where **u** is the blood velocity (m/s), **B** the magnetic flux density (T), and **L** is the distance vector across the aorta (m). This can be simplified to:

$$V=uBL\sin(\theta) \quad [2]$$

where θ is the angle between the magnetic field vector and the direction of flow. The greatest MHD voltage is induced when the magnetic field is perpendicular to the direction of flow. This relationship also indicates that the MHD signal should be linearly proportional to *B* for any subject. It should be noted that this relationship is only an estimation of induced voltages across the aorta and does not predict voltages at the body surface, which depend on factors such as torso geometry and electrode placement. In order to predict the voltages at the body surface, magnetofluid dynamics equations and a thorax model taking into account the geometry of the aorta and torso for each subject would be required (15).

Lead I is expected to have the strongest MHD effect among the 12 ECG leads due to its geometric orientation, which is approximately perpendicular to both the static magnetic field and the aortic arch. Lead I voltage is defined as the difference in potential between the left arm and right arm, while the right leg electrode is the ground. In order to minimize artifact due to limb motion during exercise, the AHA guidelines recommend an alternative placement of the limb leads on the subject's torso, as illustrated in Fig. 1.

We recorded ECG data in six healthy subjects (ages 21 to 29) lying supine on the MRI table, as well as on a table outside of the MRI room. The study protocol was approved by the institutional review board at The Ohio State University. All participants gave written informed consent. The exclusion criteria were known or suspected cardiovascular disease and the standard contraindications to MRI. In each subject, we acquired 2 min of supine ECG data, using a 12-lead ECG system (MP100A-CE; Biopac, Santa Barbara, CA) at a 1-kHz sampling rate. The Biopac system was selected to perform the data acquisition instead of the devices used for ECG gating during MRI imaging because these utilize filtering that may alter the MHD signal. The Biopac system is not MRI compatible and was positioned in the corner of the MRI room outside of the 5-G line with an ECG cable and 72-inch lead wires extending to the subject on the table. The system and lead wires were removed from the MRI room during imaging.

The measurements were performed at four to six table positions (depending on the subject's height), with the subject feet first toward the magnet, starting with the table fully extended and moving the table into the magnet bore. ECG signals were recorded at magnetic field strengths ranging from 6.4 mT to 652 mT, with the aortic arch positioned from 262 cm to 106 cm from isocenter. The subjects were instructed to remain completely still during the 2-min measurements. We also recorded the ECG of each subject while lying supine on a table outside of the MRI room to serve as a "baseline" signal with no magnetic interference.

In each subject, we acquired standard scout images to determine the location of the aortic arch relative to magnet isocenter and through-plane aortic velocity measurements perpendicular to the midarch (segmented *k*-space spoiled gradient echo, echo time/pulse repetition time 2.0/48.3 ms, 6.0mm slice, matrix 100 × 192, and rate 2 parallel acceleration). The aortic diameter at the arch and the primary direction of flow relative to the magnetic field were also determined from the phase-velocity and scout images. The phase-velocity images were also analyzed using Argus software (Siemens, Malvern, PA) to determine the peak aortic arch velocity and its timing relative to the R-wave.

Data analysis was performed using MATLAB (The Mathworks, Natick, MA). We identified the peak of each R-wave and the corresponding T-wave and segregated the data into individual RT (peak-to-peak) intervals. We rejected the RT intervals that fell outside of ±1 standard deviation of the mean RT interval duration to ensure physiologic consistency and linearly expanded or contracted the duration of each RT interval to the mean duration at baseline. We subsequently averaged all heartbeats to obtain the mean RT-interval waveform at each table position. According to the AHA exercise testing standards (11), ST displacement should be measured at 80 ms following the J-point, the transition between the QRS complex and ST segment. We visually identified the J-point for each mean waveform and analyzed the subsequent 120-ms interval; this corresponds to the estimated upper limit of the ST-segment duration (12,16).

We subtracted the baseline mean ST segment from the mean ST segment at each table position in order to determine the magnitude of the MHD effect as a function of field strength. We identified the peak MHD deviation at each position in terms of the greatest absolute voltage difference from baseline. Finally, we evaluated whether the peak deviation exceeded the AHA guideline of 0.025 mV or 5% and pooled the data from all subjects to determine the threshold at which the magnetic field begins to have a significant impact on the ECG signal.

Linear regression was performed to investigate the correlation between MHD voltages and magnetic field and between measured MHD and the aortic voltages estimated by Eq. 2 in each subject. *P* values less than an α of 0.05 were considered to indicate statistical significance.

RESULTS

The measured magnetic field of our 1.5-T MRI system as a function of distance from isocenter is displayed in Fig. 2, with vertical lines indicating the bore entrance (the plane parallel to the front panel of the magnet housing) and the end of the MRI patient table when fully extended. The bore entrance on this system was measured to be 80 cm from isocenter.

The mean RT intervals (peak to peak) in two subjects are displayed in Fig. 3a,b, with the J-point indicated on each. This figure illustrates the increasing deviation from baseline at higher magnetic field strengths. The deviation from baseline within the 120-ms interval beginning at the J-point is shown in Fig. 3c,d for the same two subjects at various magnetic field strengths. The peak deviation from baseline is plotted versus magnetic field strength in Fig. 3e,f, illustrating the linear relationship between the MHD effect and the magnetic field and the difference in slope between these two subjects. The linear relationship between field strength and MHD, as well as the timings of the J-point and peak aortic velocity for all subjects, is listed in Table 1.

The slope of the regression line between the measured MHD voltage and the aortic voltage estimated using Eq. 2 was 0.046 ± 0.038 ($r = 0.834$, $P < 0.001$). As expected, the voltage measured at the body surface was greatly attenuated compared to the estimated voltage across the aorta.

The high correlation coefficients in Table 1 within the 120-ms interval indicate that the MHD effect is linearly proportional to the magnetic field in each subject. Figure 4a displays the peak deviation from baseline for all six subjects at all measured positions. The circles indicate the points within 0.025 mV or 5%, while the squares indicate those which exceed this AHA guideline for maximum allowed signal distortion. This plot shows that all points below a magnetic field strength of 70.7 mT are within the 0.025 mV or 5% guideline. Figure 4b shows the corresponding plot of peak deviations from baseline at various positions of the aortic arch relative to the bore entrance. For the 1.5-T system used in this experiment, when the aortic arch was positioned 157 cm or more from isocenter (77 cm from the bore entrance), signal distortion was within the 0.025 mV or 5% guideline for all subjects.

DISCUSSION AND CONCLUSIONS

The aim of this study was to determine the magnetic field threshold for accurate ECG monitoring inside the MRI room. We have shown that reliable ECG measurements can be obtained within the ST segment at magnetic field strengths below approximately 70 mT measured at the aortic arch in supine subjects. With knowledge of the magnetic field plot of a particular MRI room, obtained either through gauss-meter measurements or from magnet manufacturer specifications, it is possible to determine the location relative to the MRI system that defines the 70-mT threshold. For the 1.5-T MRI system used in this study, this distance is approximately 160 cm from the isocenter and 80 cm from the magnet bore entrance.

With the table fully extended and the subjects positioned feet first toward the magnet, the closest aortic arch distance to the isocenter was 262 cm, well outside the 160-cm limit, indicating that accurate ECG measurements are feasible in the feet-first orientation. With the table fully extended and the patient positioned headfirst toward the magnet and the head positioned at the bore entrance, the aortic arch would typically lie within 160 cm of the isocenter, and distortions of the ECG signal may exceed AHA guidelines. However, accurate ECG recording may still be possible with the patient lying headfirst on the extended patient table, provided that care is taken to position the patient as far away from the magnet as possible. This would, of course, depend on the length of the extended patient table and the fringe field of the particular MRI system. We anticipate that accurate ECG recording should be feasible for general patient monitoring inside the MRI room, during supine bicycle exercise on the fully extended MRI table, during exercise on a treadmill positioned adjacent to the MRI table, and during recovery on the MRI table following exercise or pharmacologic stress testing. Although the peak aortic flow and the static magnetic field would be oriented differently during upright bicycle or treadmill exercise, our measurements represent the worst-case scenario, with the flow velocity, the static magnetic field, and the ECG lead all approximately perpendicular to each other. Whereas other segments of the aorta may be oriented perpendicular to the magnetic field when standing or sitting, the flow velocities do not vary appreciably, with average velocities of 104, 101, and 113 cm/sec in the ascending, descending, and abdominal aorta, respectively (13).

The AHA guidelines specify that an acceptable threshold for ECG signal distortion due to filtering is 0.025 mV or 5%, whichever is greater. Due to the low voltages within the ST segment, 0.025 mV was the higher threshold in each case. This AHA standard defines the limit of distortion introduced by filtering as the maximum allowed deviation from the true waveform. However, in this experiment we encountered the additional factor of physiologic variability between measurements at different table positions. For example, subjects may have experienced excitation or stress, altering signal amplitudes and timing. Heart rates and breathing patterns were observed to change in some instances. These physiologic changes may have introduced distortion of the ECG relative to the baseline signal unrelated to the MHD effect. Any change relative to baseline was grouped with the MHD effect, and we may thus be conservative in our assessment of the static field limit. Two minutes of data (~100 heartbeats) were averaged to suppress noise and respiratory motion artifact, and temporal normalization methods were employed to minimize the effect of heart-rate variability.

The peak blood flow velocity in the aortic arch was found to occur between 109 ms and 144 ms following the R-wave in the six subjects. Since the J-point occurred no later than 54 ms following the R-wave, the peak blood flow velocity in these subjects occurred within the ST segment. We evaluated every point within the ST segment in 1-ms increments and determined the maximum MHD effect. The peak deviation from the baseline ECG did not occur at the same time point at the different field strengths in each subject due to physiologic variability.

The MHD effect for each subject was linearly proportional to the magnetic field strength. The MHD plots for different subjects, such as Fig. 3e and f, had different slopes due to the variability in aortic velocity, aortic arch angle and diameter, torso size, and electrode placement. While the estimated voltages across the aorta and the measured induced voltages at the body surface were linearly correlated ($r = 0.834$, $P < 0.001$), Eq. 2 is an oversimplification and cannot account for the thoracic geometry and the complex nature of blood flow in the heart and thoracic vasculature.

The average resting supine peak aortic flow velocity in our subjects (86 cm/sec) was approximately equal to the average peak aortic velocity (80 cm/sec) measured in subjects in the 50- to 74-year age range immediately following maximal treadmill exercise (17). Therefore, these data acquired in young healthy subjects should extrapolate to the typical cardiac patient cohort under stress conditions. At reduced cardiac output and flow velocities, the MHD effects would only be lower than those we observed.

One limitation of this work is that we only investigated ECG distortion in normal subjects and did not examine how the MHD may mask or mimic pathologic changes in the ST segment. Experiments are planned to examine patients with chronic myocardial infarction and existing ST-segment changes to determine whether these abnormalities can be reliably detected at magnetic fields <70 mT. Another potential limitation may be translating the static field limit to MRI systems with sharp static gradients in the fringe field. In the presence of a steep field gradient, motion of the torso due to breathing may induce voltages in the ECG leads. In the feet-first orientation in which the measurements were performed, lead I was approximately at the level of the aortic arch and was thus positioned at the location where the field strength was measured. The ECG was averaged over 2 min; while the MHD effect is expected to be static across cardiac cycles and not affected by averaging, changes in the ECG caused by respiratory motion would be dynamic and suppressed by the averaging process. This indicates that the distortion we detected was indeed caused by MHD effects and was not a result of motion of leads positioned in a steep gradient. Given an approximate distance of 30 cm between the aortic arch and the lowest electrodes on the torso (right leg, left leg), in a feet-first position it is possible that some leads fall within a sharp magnetic field gradient and experience motion-induced signal distortion even when the aortic arch is outside of the static threshold. This would depend on the fringe field of the particular MRI system. Although the conclusions pertaining to lead I should not be affected, care should be taken when translating the findings to the other nine leads. Conversely, in the headfirst orientation, lead I represents the worst-case scenario, being closest to the bore. All other leads would be positioned at lower field strengths (<70 mT) and lower static field gradients. In addition, it should be noted that the fringe field of 3 T and higher field systems is likely to extend farther from the bore entrance and potentially have sharper static field gradients than 1.5 T.

Acknowledgments

The authors acknowledge Dennis E. Mathias for the graphic design in Fig. 1, Dr. Petra Schmalbrock for the use of her gaussmeter, and Dr. Robert Hamlin for the use of his Biopac signal recorder.

References

1. Nijm GM, Swiryn S, Larson AC, Sahakian AV. Extraction of the magnetohydrodynamic blood flow potential from the surface electrocardiogram in magnetic resonance imaging. Med Biol Eng Comput. 2008; 46:729–733. [PubMed: 18239947]
2. Fischer SE, Wickline SA, Lorenz CH. Novel real-time R-wave detection algorithm based on the vectorcardiogram for accurate gated magnetic resonance acquisitions. Magn Reson Med. 1999; 42:361–370. [PubMed: 10440961]
3. Myers J, Arena R, Franklin B, Pina I, Kraus WE, McInnis K, Balady GJ. Recommendations for clinical exercise laboratories: a scientific statement from the American Heart Association. Circulation. 2009; 119:3144–3161. [PubMed: 19487589]
4. Kramer M, Barkhausen J, Flamm SD, Kim RJ, Nagel E. Standardized cardiovascular magnetic resonance imaging (CMR) protocols, Society for Cardiovascular Magnetic Resonance: Board of Trustees Task Force on Standardized Protocols. J Cardiovasc Magn Reson. 2008; 10:35. [PubMed: 18605997]
5. Cheng CP, Schwandt DF, Topp EL, Anderson JH, Herfkens RJ, Taylor CA. Dynamic exercise imaging with an MR-compatible stationary cycle within the general electric open magnet. Magn Reson Med. 2003; 49:581–585. [PubMed: 12594764]
6. Chiribiri A, Bettencourt N, Nagel E. Cardiac magnetic resonance stress testing: results and prognosis. Curr Cardiol Rep. 2009; 11:54–60. [PubMed: 19091176]
7. Hjortdal VE, Emmertsen K, Stenbog E, Frund T, Schmidt MR, Kromann O, Sorensen K, Pedersen EM. Effects of exercise and respiration on blood flow in total cavopulmonary connection: a real-time magnetic resonance flow study. Circulation. 2003; 108:1227–1231. [PubMed: 12939218]
8. Jekic M, Foster EL, Ballinger MR, Raman SV, Simonetti OP. Cardiac function and myocardial perfusion immediately following maximal treadmill exercise inside the MRI room. J Cardiovasc Magn Reson. 2008; 10:3. [PubMed: 18272005]
9. Rerkpattanapipat P, Gandhi SK, Darty SN, Williams RT, Davis AD, Mazur W, Clark HP, Little WC, Link KM, Hamilton CA, Hundley WG. Feasibility to detect severe coronary artery stenoses with upright treadmill exercise magnetic resonance imaging. Am J Cardiol. 2003; 92:603–606. [PubMed: 12943887]
10. Tavel ME. Stress testing in cardiac evaluation: current concepts with emphasis on the ECG 10. Chest. 2001; 119:907–925. [PubMed: 11243976]
11. Fletcher GF, Balady GJ, Amsterdam EA, Chaitman B, Eckel R, Fleg J, Froelicher VF, Leon AS, Pina IL, Rodney R, Simons-Morton DA, Williams MA, Bazzarre T. Exercise standards for testing and training: a statement for healthcare professionals from the American Heart Association. Circulation. 2001; 104:1694–1740. [PubMed: 11581152]
12. Simonson E, Cady LD Jr, Woodbury M. The normal Q-T interval. Am Heart J. 1962; 63:747–753. [PubMed: 13913188]
13. Wilson N, Goldberg SJ, Dickinson DF, Scott O. Normal intracardiac and great artery blood velocity measurements by pulsed Doppler echocardiography. Br Heart J. 1985; 53:451–458. [PubMed: 3986059]
14. Bailey JJ, Berson AS, Garson A Jr, Horan LG, Macfarlane PW, Mortara DW, Zywietz C. Recommendations for standardization and specifications in automated electrocardiography: bandwidth and digital signal processing: a report for health professionals by an ad hoc writing group of the Committee on Electrocardiography and Cardiac Electro-physiology of the Council on Clinical Cardiology, American Heart Association. Circulation. 1990; 81:730–739. [PubMed: 2297875]
15. Gupta A, Weeks AR, Richie SM. Simulation of elevated T-waves of an ECG inside a static magnetic field (MRI). IEEE Trans Biomed Eng. 2008; 55:1890–1896. [PubMed: 18595808]

16. Draper HW, Peffer CJ, Stallmann FW, Littmann D, Pipberger HV. The corrected orthogonal electrocardiogram and vectorcardiogram in 510 normal men (Frank lead system). Circulation. 1964; 30:853–864. [PubMed: 14246330]
17. Lazarus M, Dang TY, Gardin JM, Allfie A, Henry WL. Evaluation of age, gender, heart rate and blood pressure changes and exercise conditioning on Doppler measured aortic blood flow acceleration and velocity during upright treadmill testing. Am J Cardiol. 1988; 62:439–443. [PubMed: 2970778]

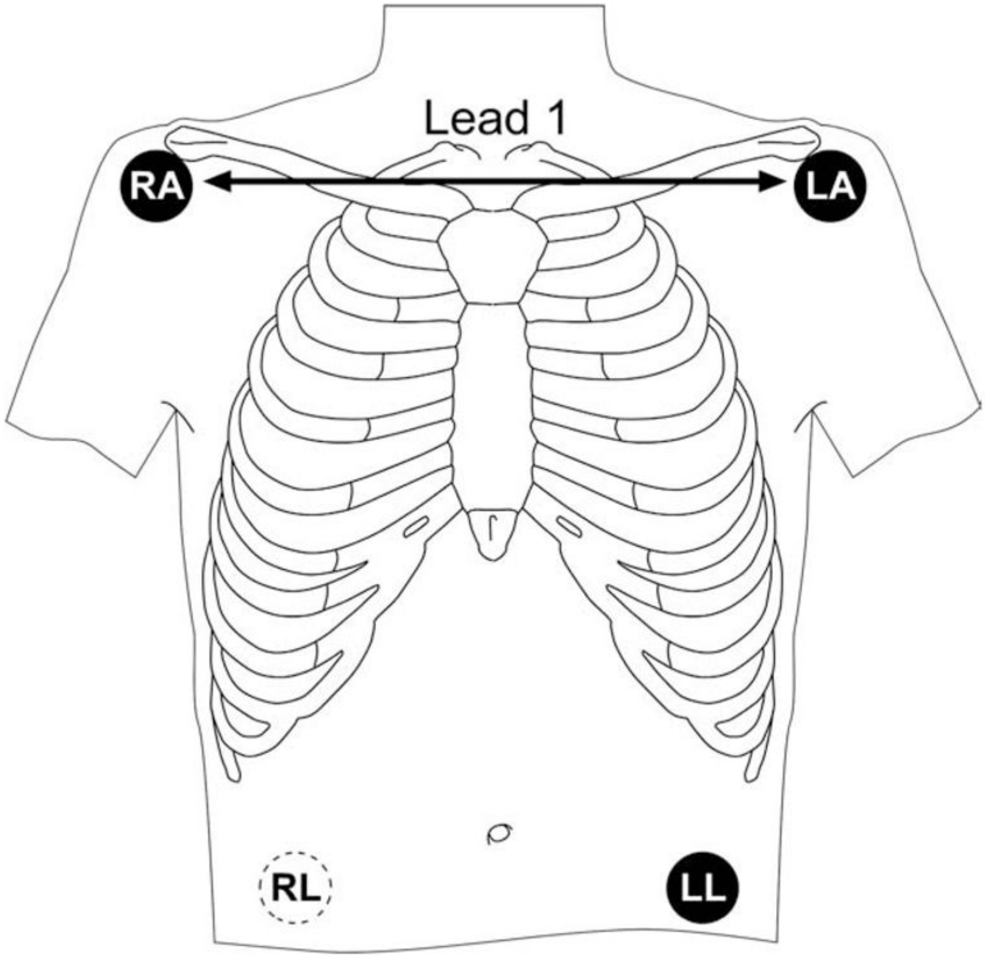

FIG. 1.
Electrode placement for lead I of a 12-lead ECG.

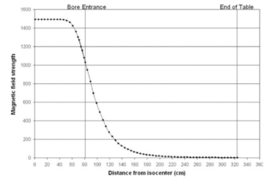

FIG. 2.

Measured magnetic field of the 1.5-T Siemens Avanto as a function of distance from the isocenter.

NIH-PA Author Manuscript
NIH-PA Author Manuscript

NIH-PA Author Manuscript
NIH-PA Author Manuscript

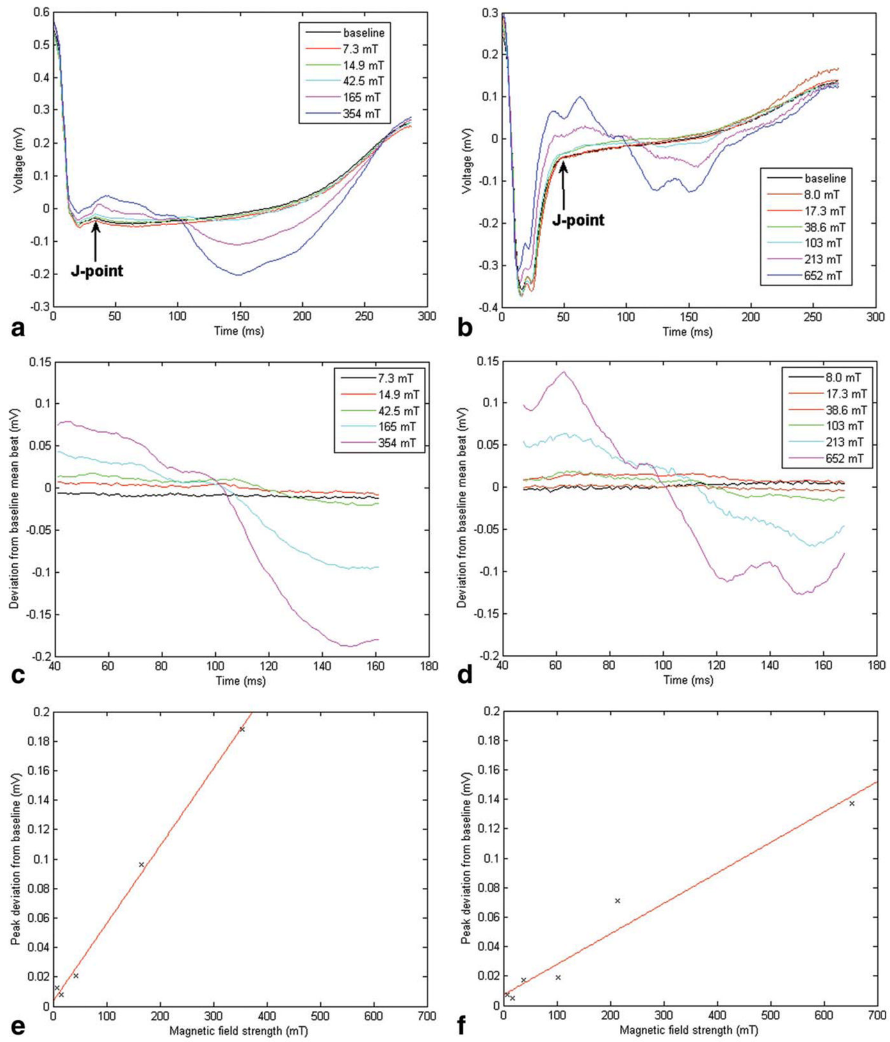

FIG. 3.

a,b: Mean RT intervals (peak to peak) in two subjects outside the MRI room (baseline) and at various magnetic field strengths. The J-point is shown (arrow). **c,d:** The corresponding deviation from baseline at different field strengths within a 120-ms interval following the J-point. **e,f:** Peak deviation from baseline as a function of field strength, indicating a linear relationship between the MHD effect and the magnetic field and a difference in slope between the two subjects.

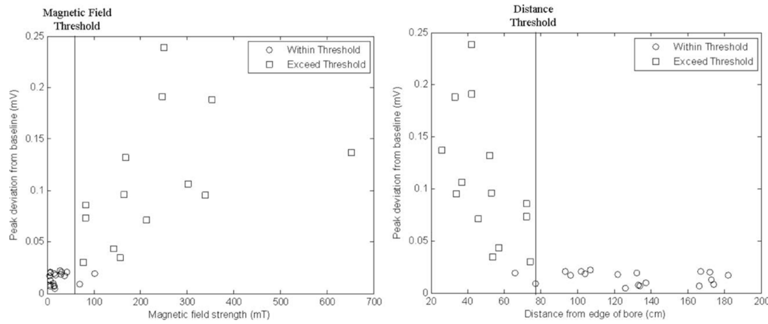

FIG. 4.

a: Peak deviation from baseline for all six subjects expressed as a function of magnetic field strength. Below the field strength of 70 mT, peak deviation is below 0.025 mV in all subjects. **b:** Peak deviation from baseline expressed as a function of the distance of the aortic arch from the bore entrance. At distances of 80 cm or more from the bore, peak deviation is below 0.025 mV in all subjects.

Table 1

Time Following the R-Wave When the J-Point Occurred, the Correlation Coefficient Indicating a Linear Relationship Between the MHD Effect and the Magnetic Field Strength, the Slope of the Curve Representing the Deviation From Baseline as a Function of the Magnetic Field Strength, and the Peak Velocity in the Aortic Arch and Its Timing Relative to the R-Wave for the Six Subjects

Subject	J-point (ms)	Time of peak velocity in aortic arch (ms)	Peak velocity in aortic arch (cm/sec)	Correlation coefficient	Slope (mV/T)
1	50	144	102	0.997, $P = 0.0026$	0.936
2	49	129	66	0.952, $P = 0.0034$	0.308
3	40	121	71	0.998, $P < 0.001$	0.523
4	54	144	93	0.981, $P < 0.001$	0.252
5	47	109	85	0.980, $P < 0.001$	0.206
6	50	97	98	0.992, $P < 0.001$	0.742